JOURNAL OF MATERIALS SCIENCE 31 (1996) 4957–4966

Characterization of the cavity nucleation factor for life prediction under creep–fatigue interaction

BAIG GYU CHOI, SOO WOO NAM
Department of Materials Science and Engineering, Korea Advanced Institute of Science and Technology, 373-1 Kusong-dong, Yusong-gu, Taejon, Korea

YOUNG CHEOL YOON
Research & Development Team, Technology Center, SamSung Motors Inc. Banwol-ri, Taean-eup, Hwasung-kun, Kyungki-do, Korea

JOONG JAE KIM
Department of Automotive Engineering, Halla Institute of Technology, Heungup-li, Heungup-myon, Wonju-si, Kangwon-do, Korea

It is understood that grain boundary cavitation is one of the detrimental processes for the degradation of materials that reduces the creep–fatigue life at high temperatures. In a previous investigation, a model for life prediction under creep–fatigue conditions was proposed in terms of cavity nucleation and growth. In that model, the cavity nucleation factor (P) was introduced to correlate between the number of cavities and the plastic strain range from which athermal vacancies are generated. It was considered to be a material specific constant which was independent of the experimental conditions. However, in this study, it is found that the cavity nucleation factor is a function of the plastic strain range but is independent of the testing temperature at near 0.5 T_m. In the light of this dependency, a new cavity nucleation factor (P'), is introduced. Using this new cavity nucleation factor (P'), a modified equation for life prediction is proposed, and it is shown that there is good agreement between predicted and experimental lives. Additionally, an interesting approach has been made to find the physical meaning of the new cavity nucleation factor (P'). According to this study, it is suggested that the new cavity nucleation factor, which is regarded as a material specific constant, is found to be strongly related to the density of the grain boundary precipitates with a linear relationship existing between them.

1. Introduction

A high temperature low cycle fatigue experiment with a tensile hold time at the peak tensile strain (creep–fatigue interaction) is one of the tests for understanding life limiting phenomena in many components used in power generation and aeronautics. In the study of creep–fatigue interaction, the quantification and prediction of fatigue lives are important. Therefore, it is important to have a reliable method for life prediction, and an understanding of the micromechanistic damage formation mechanism. Two models have been suggested on the basis of micromechanistic considerations for life prediction under combined creep–fatigue damage conditions. One model is proposed by Tomkins and Wareing [1] and the other is by Majumdar and Maiya [2]. The practical application of these models, however, is difficult since many of the various parameters and constants in the equations are not readily available.

Recently, Hong and Nam [3] have proposed a model for the prediction of the fatigue life of a material, in which the creep cavitational damage is dominant under creep–fatigue cycling. They showed that the model could predict the creep–fatigue life fairly accurately if the failure is controlled by cavitation damage on grain boundaries rather than by a process of fatigue crack initiation and propagation. However, they could only use the data for several alloys over one or two strain ranges for checking the reliability of the model. Later on, when results from many more strain range tests became available the present investigators discovered that not all the predicted lives agreed with the test results.

In this work, using the expanded experimental data base of several strain range and temperature tests, it is attempted to correct the deficiency in the model by characterizing the dependency on the plastic strain range of the cavity nucleation factor and to propose a modified equation for life prediction applicable to the creep–fatigue interaction. In addition we attempt to find a physical representation for the cavity nucleation factor which is introduced to modify the model.

2. A review of the existing model

It is worthwhile to review the previous grain boundary cavity damage based model [3] for life prediction under low-cycle fatigue conditions with a hold time at

0022–2461

the tensile peak strain. It was assumed that mechanically generated vacancies form cavities during the tensile lamp of fatigue (fatigue effect) and then grow during the tensile hold time period (creep effect) thereby creating the creep–fatigue interaction.

The model explained that vacancies were formed by plastic deformation during the fatigue cycle and clustered to form cavities on the grain boundaries. It was assumed that the number of cavities formed in a cycle was proportional to the plastic strain range. Therefore, the number of nucleated cavities during cyclic loading per unit area of grain boundary, n, was assumed to be

$$n = P\Delta\varepsilon_p N \quad (1)$$

where P, $\Delta\varepsilon_p$ and N were the cavity nucleation factor, the plastic strain range, and the number of cycles, respectively.

These generated cavities were assumed to grow during the hold time period at the tensile peak strain by grain boundary diffusion of the vacancies. The Hull–Rimmer model [4] for diffusional growth of cavities at a grain boundary was incorporated into the model in order to provide a good approximation for the cavity growth, but the stress term of the original Hull–Rimmer equation had to be modified as a function of hold time because of the load relaxation taking place during the tensile hold time in the creep–fatigue interaction. The equation is now formulated as;

$$\frac{dA}{dt} = \frac{2\pi\delta D_g \Omega \sigma(t)}{kTl} \quad (2)$$

where A was the cavitated area of a given cavity, l was the cavity spacing, D_g was the grain boundary diffusivity, Ω was the atomic volume, $\sigma(t)$ was the peak tensile stress relaxation term during hold time, and k and T have their usual meanings.

It was assumed that the same process was repeated throughout the fatigue cycling until the total cavitated area on the grain boundaries reached its critical value. The expression for the total cavitated area is given by;

$$A_t = \frac{2}{5} P^{3/2} \Delta\varepsilon_p^{3/2} N^{5/2} \frac{2\pi\delta D_g \Omega}{kT} \int_0^t \sigma(t)\,dt \quad (3)$$

The failure due to the creep–fatigue interaction was assumed to be controlled by creep cavitational damage rather than by a process of fatigue crack initiation and propagation. At a critical number of cycles to failure (N_{cr}), up to which the above mentioned processes were continuously taking place, it was assumed that the load carrying capacity was drastically reduced by coalescence of grain boundary cavities and unstable crack growth was begun. Thus from Equation 3 the number of cycles to failure can be written as

$$N_{cr} = C(P\Delta\varepsilon_p)^{-3/5} \left\{ \frac{\exp(-Q_g/RT)}{T} \int_0^t \sigma(t)\,dt \right\}^{-2/5} \quad (4)$$

where,

$$C = \left(\frac{4\pi\Omega\delta D_0}{5kA_t} \right)^{-2/5}$$

where Q_g is the activation energy of grain boundary diffusion, P is the cavity nucleation factor and C is a constant including the critical cavitated area (A_t). In this equation, it was assumed that the creep–fatigue life was controlled solely by the cavitational damage and the failure occurred at the critical value of A_t. Therefore, A_t was regarded as a constant in the model. To obtain the critical value of A_t, the failure criterion had to be preferentially determined. In this model, it was assumed that failure occurred on cavity linkage when the radius of a cavity was equal to half of the spacing between the centre of cavities in its periodic array, a condition which was suggested by Raj and Ashby [5] and other investigators [6, 7]. From this assumption for the failure criterion, the final value of A_t was obtained to be 0.7854 as follows:

$$A_t = \frac{\pi\gamma^2}{l^2} = 0.7854, \quad \text{when } r = \frac{l}{2} \quad (5)$$

Taking the above result into consideration, the application of the life prediction method can be described as follows; from an experimental result at any condition (i.e. a specific temperature, strain range and tensile hold time) P in Equation 4 was obtained as a material-dependent constant in order to make the predicted and experimental lives the same. Using this calculated value of P, the creep–fatigue lives with other strain ranges and hold times were then calculated.

This equation for life prediction was checked with other investigators' experimental results obtained over a limited range of strain conditions, and it was shown that the predicted creep–fatigue lives were in good agreement with the experimentally observed ones for AISI 304 and AISI 316 stainless steels over various hold time periods. However, the available data used for checking the reliability of the model was very limited, in that, creep–fatigue results over only one or two strain ranges were applied. Thus the use of this model in systems under different strain ranges will remain controversial until the model has been tested with considerable amount of data over several strain ranges. Therefore, in this paper, we check the reliability of the model over a wide range of strain range conditions, and attempt to modify the original model so that it is applicable to more general cases.

3. Results and discussion

3.1. Modified model for creep–fatigue life prediction

Even though numerous test results for the creep–fatigue interaction have been published, only a limited number of data sets [8, 9] could be used to calculate the predicted fatigue life from Equation 4, simply because only those data have the values of the stress relaxation during hold time which is used in the integral term in the equation.

Ermi and Moteff [8] performed creep–fatigue tests on AISI 304 stainless steel at 866K and Brinkman *et al.* [9] independently conducted tests on AISI 316 stainless steel at 866K. Their creep–fatigue data are

TABLE I Creep–fatigue test data for AISI 304 stainless steel tested at 866 K [8]

$\Delta\varepsilon_t$ (%)	$\Delta\varepsilon_p$ (%)	t_h (min)	$\int \sigma\, dt$ (MPa sec)	N_{exp}
± 2.05	1.68	1	15674.6	398
± 1.98	1.66	60	777846	112
± 2.02	1.74	180	2164900	63
± 1.00	0.70	1	13228.4	1748
± 1.00	0.72	10	117107	706
± 0.99	0.72	60	671346	338
± 1.02	0.76	180	1871670	170
± 0.50	0.29	1	9820.1	10406
± 0.55	0.34	60	487171	1253

$Q_g = 195\ kJ\ mol^{-1}$ [13]

TABLE II Creep–fatigue test data for AISI 316 stainless steel tested at 866 K [9]

$\Delta\varepsilon_t$ (%)	$\Delta\varepsilon_p$ (%)	t_h (min)	$\int \sigma\, dt$ (MPa sec)	N_{exp}
± 2.0	1.641	6	134011	71
± 2.0	1.623	6	131282	115
± 1.99	1.641	30	619147	57
± 2.0	1.621	30	576966	64
± 2.0	1.741	60	1063870	43
± 2.0	1.691	309.6	4620900	25
± 2.0	1.755	600	8514160	15
± 1.0	0.602	6	101683	393
± 1.0	0.592	6	114032	438
± 0.98	0.655	30	523763	221
± 1.0	0.727	300	3998340	84
± 0.5	0.164	6	83430.5	1985
± 0.5	0.209	30	390828	1050

$Q_g = 187\ kJ\ mol^{-1}$ [13]

shown in Tables I and II, respectively. Only these data sets are known to contain all the information we require.

Fig. 1 shows a comparison between the experimental lives obtained from the creep–fatigue test results of Ermi and Moteff [8] on AISI 304 stainless steel and the predicted lives calculated from Equation 4. In this case, the cavity nucleation factor, P, in Equation 4 is calculated so as to make the predicted and experimental lives the same for a given test condition of the total strain range of ± 1.0% at a tensile hold time of 10 min. Using this calculated value of P, the fatigue lives of all the other experimental conditions could be calculated and be compared with the experimentally measured equivalent fatigue lives.

From Fig. 1, the differences between the predicted lives and the experimentally measured lives can be observed, and the trend in the deviation is very distinctive. Regardless of any variation in the hold time, for the same strain range it is found that the predicted lives are in reasonable agreement with the experimental lives. As can be seen a systematic deviation marked by the dotted lines in the Fig. 1, exists, if the strain range differs from that of the reference condition (i.e. the strain range which is used to calculate the value of P). If the strain range is greater than the

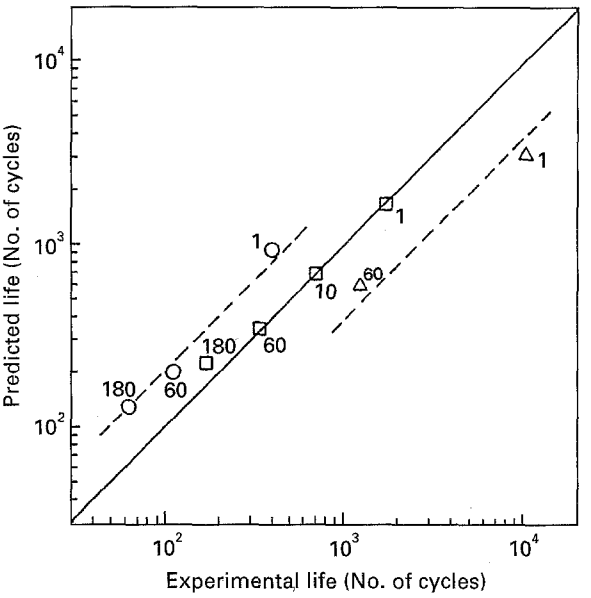

Figure 1 Comparison between predicted lives calculated from Equation 4 and experimental lives of AISI 304 stainless steel by Ermi and Moteff [8]. The data were taken at 866 K and (○) $\Delta\varepsilon_t = \pm 2.0\%$, (□) $\Delta\varepsilon_t = \pm 1.0\%$ and (△) $\Delta\varepsilon_t = 0.5\%$.

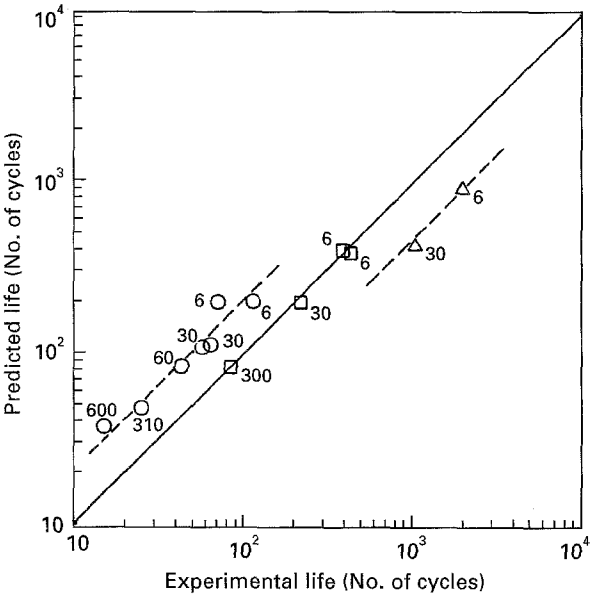

Figure 2 Comparison between predicted lives calculated from Equation 4 and experimental lives of AISI 316 stainless steel by Brinkman *et al.* [9]. The data were taken at 866 K and (○) $\Delta\varepsilon_t = \pm 2.0\%$, (□) $\Delta\varepsilon_t = \pm 1.0\%$ and (△) $\Delta\varepsilon_t = \pm 0.5\%$.

reference condition then an overestimation of life prediction is observed whilst if it is smaller, then an underestimation is observed. Of interest is the observation that a graph of the deviations in the predicted life shows that they tend to be parallel straight lines. To see if this is a general phenomenon, the results of creep–fatigue tests obtained by Brinkman *et al.* [9] in 316 stainless steel are used for comparison purposes. The reference experimental condition used to calculate the value of the cavity nucleation factor, P, is a total strain range of ± 1.0% and a tensile hold time of 300 min. As shown in Fig. 2, a similar consistent deviation for the predicted lives is also observed for this alloy.

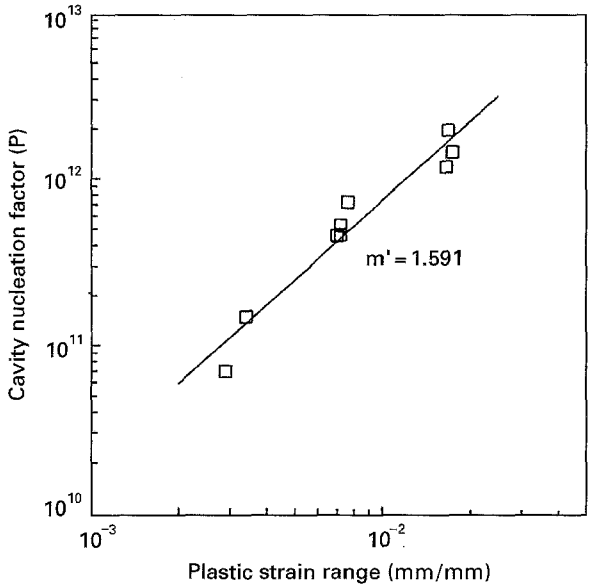

Figure 3 Variation of cavity nucleation factor with plastic strain range in AISI 304 stainless steel by Ermi and Moteff [8].

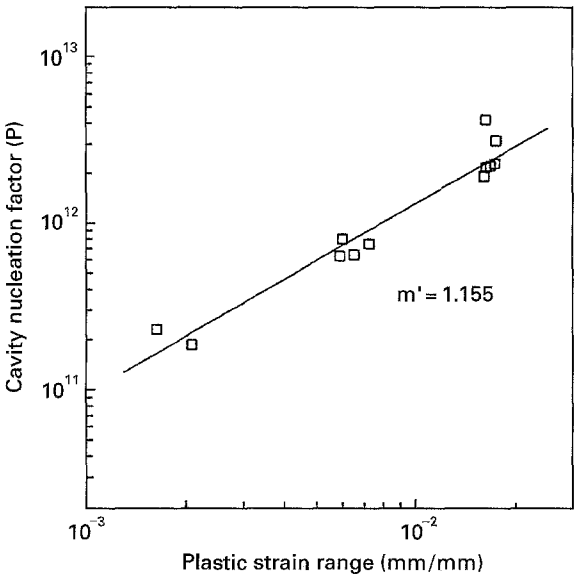

Figure 4 Variation of cavity nucleation factor with plastic strain range in AISI 316 stainless steel by Brinkman *et al.* [9].

From the above analysis, it is clear that this phenomenon in the deviation behaviour is due to a failing in the model. Therefore, to predict the fatigue life more reliably, Equation 4 of the model must be corrected.

To find the reason for the deviation with strain range of the predicted life, the dependency on the strain range of each term in Equation 4 has to be considered. In Equation 4, those terms obtained experimentally (i.e. plastic strain range, temperature and integration of stress relaxation) and other constant terms (i.e. activation energy for grain boundary diffusion and gas constant) are not related to the plastic strain range but fixed values. As has already been seen from Figs 1 and 2 the cavity nucleation factor, P, in Equation 4 is assumed to be the only term which may vary depending on the strain range. To observe any possible dependence of the cavity nucleation factor on the strain range, the values of P are recalculated to make the predicted lives equal to the experimental lives for all the data. Figs 3 and 4 indicate the variation in the values of P with plastic strain range in AISI 304 and 316 stainless steels, respectively. From these figures one can see that the value of P is strongly dependent on the plastic strain range, i.e. as the plastic strain range increased, the calculated values of P increased. And a linear relationship between them is obtained in a log-log plot. As a result, it is found that the cavity nucleation factor, which has been considered as a material constant, is no longer a material constant but depends on the plastic strain range. Therefore, the previously suggested cavity nucleation factor in Equation 1 must be modified as a function of the plastic strain range, i.e.,

$$P = P' \cdot \Delta\varepsilon_p^{m'} \tag{6}$$

where P' is a new cavity nucleation factor regarded as a real material constant and m', whose value indicates the degree of dependency on the plastic strain range of P, is a slope in Figs 3 and 4.

Substituting Equation 6 into Equation 1, the number of cavities in a cycle can be represented by the

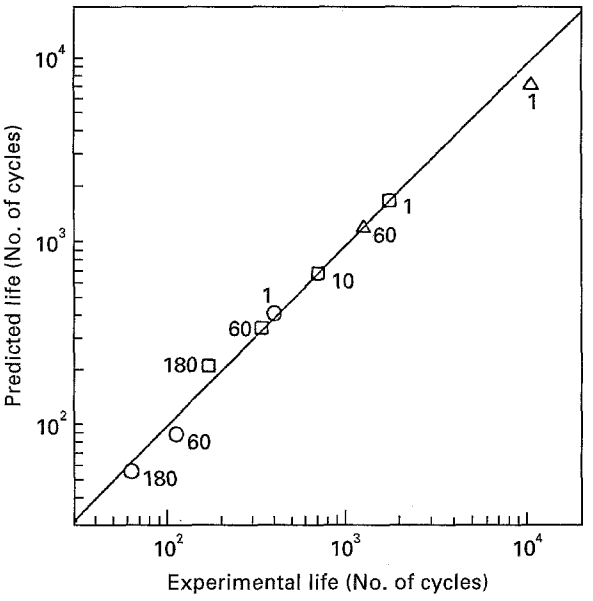

Figure 5 Comparison between predicted lives calculated from Equation 8 and experimental lives for AISI 304 stainless steel by Ermi and Moteff [8]. The data was recorded at 866 K and (○) $\Delta\varepsilon_t = \pm 2.0\%$, (□) $\Delta\varepsilon_t = \pm 1.0\%$ and (△) $\Delta\varepsilon_t = \pm 0.5\%$.

equation

$$n = P'\Delta\varepsilon_p^{m} \cdot N \tag{7}$$

where $m = m' + 1$. Using this expression, one may obtain the new equation for life prediction in terms of the new cavity nucleation factor, P',

$$N_{cr} = C(P'\Delta\varepsilon_p^{m})^{-3/5} \left\{ \frac{\exp(-Q_g/RT)}{T} \int_0^t \sigma(t)\,dt \right\}^{-2/5} \tag{8}$$

where C is a constant whose value is represented by Equation 4.

Using the results of the fatigue tests and the parameters in Equation 6, a comparison between the predicted and the experimental lives is conducted and the results are shown in Figs 5 and 6 for AISI 304 and 316

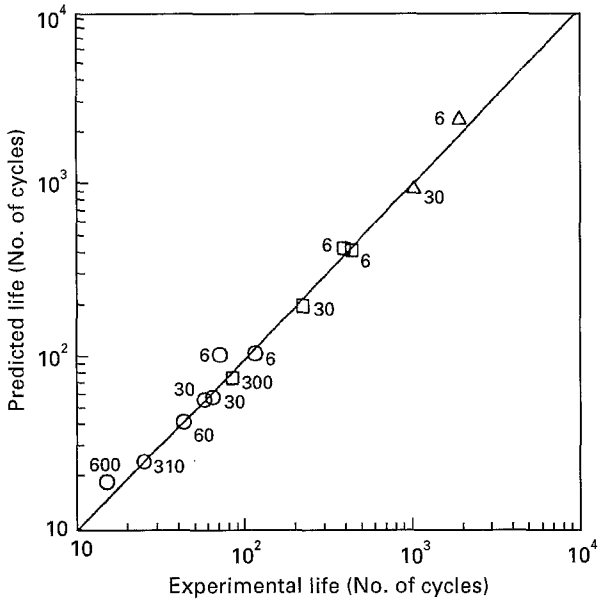

Figure 6 Comparison between predicted lives calculated from Equation 8 and experimental lives for AISI 316 stainless steel by Brinkman *et al.* [9]. The data was recorded at 866 K with; (○) $\Delta\varepsilon_t = \pm 2.0\%$, (□) $\Delta\varepsilon_t = \pm 1.0\%$ and (△) $\Delta\varepsilon_t = \pm 0.5\%$.

stainless steels [8, 9], respectively. The predicted lives are found to be in good agreement with the experimental ones. This excellent agreement between the predicted and observed fatigue lives over the several strain range tests strongly suggests that the corrected model of the cavitation damage during fatigue is believed to be physically feasible and is accepted as a general expression.

3.2. Temperature dependence of the cavity nucleation factor

In the previous section, the creep–fatigue test results obtained at only one temperature were used to consider the dependence of the cavity nucleation factor on the strain range. However, since it is known that the temperature is one of the important factors that affect the fatigue life, one needs to know whether the cavity nucleation factor in this model is also affected by the temperature. Therefore, it is necessary to check the dependence of cavity nucleation factor on the temperature.

The data used to check the temperature effect are the creep–fatigue results for AISI 304 stainless steel at 823, 873 and 898 K conducted in our laboratory. This alloy is damaged by grain boundary cavitation under the creep–fatigue interaction condition [10]. Jaske *et al* [11] performed the creep–fatigue test on Incoloy 800 at 811 and 922 K. Incoloy 800 is a high Ni-containing austenitic stainless steel, in which the main damage under creep–fatigue loading condition is also grain boundary cavitation as classified by Ostergren [12]. Thus, it is valid to use the test results of Incoloy 800 to check the reliability of this model. From the above considerations, two sets of data are used to check the temperature dependence of the cavity nucleation factor, and those data are listed in Tables III and IV for AISI 304 stainless steel and Incoloy 800 [11], respectively.

Fig. 7 shows the comparison between the experimental lives obtained from the creep–fatigue test results for AISI 304 stainless steel by the authors and the predicted lives calculated from Equation 4. Regardless of the temperature variation, for a similar plastic strain range it is found that the predicted lives agree reasonably with the experimental lives. As described in the previous section, the deviation of the predicted lives against the experimental lives is caused by a difference of the plastic strain range. Fig. 8 shows the dependence of the cavity nucleation factor on the plastic strain range for AISI 304 stainless steel. In this figure, it can be found that the cavity nucleation factor does not depend on the temperature, but only depends on the plastic strain range.

Similar results can be obtained for Incoloy 800 [11]. As shown in Figs 9 and 10, the deviation of the predicted lives against the experimental lives is also

TABLE III Creep–fatigue test data for AISI 304 stainless steel

Temperature	$\Delta\varepsilon_t$ (%)	$\Delta\varepsilon_p$ (%)	t_h (min)	$\int \sigma\, dt$ (MPa sec)	N_{exp}
	± 2.0	1.641	10	180040	556
823 K	± 2.0	1.688	30	566080	357
	± 2.0	1.714	60	1167200	261
	± 2.0	2.03	10	127530	310
	± 1.5	1.14	10	98875	600
	± 1.5	0.89	10	90955	700
	± 1.0	0.63	10	81009	1100
873 K	± 2.0	2.05	30	388010	174
	± 1.5	0.98	30	217100	498
	± 1.0	0.68	30	208700	796
	± 2.0	2.06	60	899957	140
	± 2.0	2.226	10	101180	222
898 K	± 2.0	2.310	30	318600	145
	± 2.0	2.330	60	792500	97
$Q_g = 195\ \text{kJ mol}^{-1}$ [13]					

TABLE IV Creep–fatigue test data for Incoloy 800 stainless steel [11]

Temperature	$\Delta\varepsilon_t$ (%)	$\Delta\varepsilon_p$ (%)	t_h (min)	$\int \sigma \, dt$ (MPa sec)	N_{exp}
811 K	± 2.26	1.59	10	222367	464
	± 2.24	1.71	10	205410	412
	± 0.53	0.19	10	186168	5400
	± 2.39	1.80	60	1738230	202
	± 2.38	1.82	60	1430840	205
	± 2.38	1.90	300	8096740	66
922 K	± 2.00	1.55	10	129837	128
	± 0.54	0.29	10	137777	980
	± 0.54	0.34	10	137114	850
	± 2.39	1.98	60	1010240	49
	± 2.43	2.01	60	869830	50
	± 0.53	0.38	60	584115	310
	± 2.37	1.96	300	4262140	40

$Q_g = 179.9 \text{ kJ mol}^{-1}$ [13]

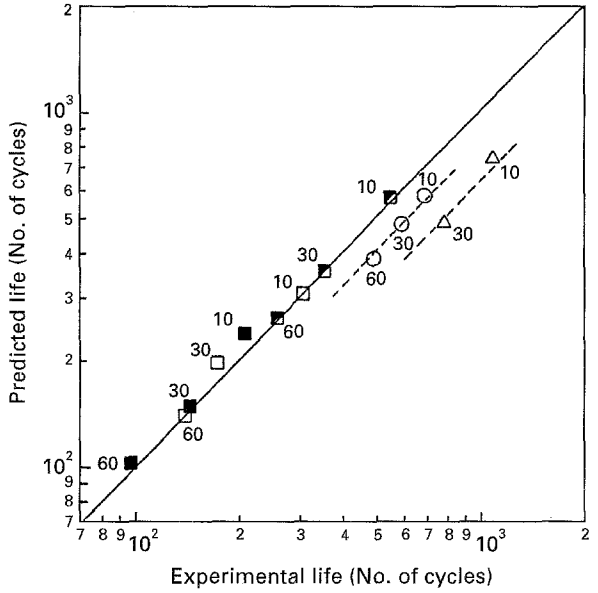

Figure 7 Comparison between predicted lives calculated from Equation 4 and experimental lives for AISI 304 stainless steel. The data was recorded at (◩) 823 K, (□) 873 K and (■) 898 K with (□) $\Delta\varepsilon_t = \pm 2.0\%$, (○) $\Delta\varepsilon_t = \pm 1.5\%$ and (△) $\Delta\varepsilon_t = \pm 1.0\%$.

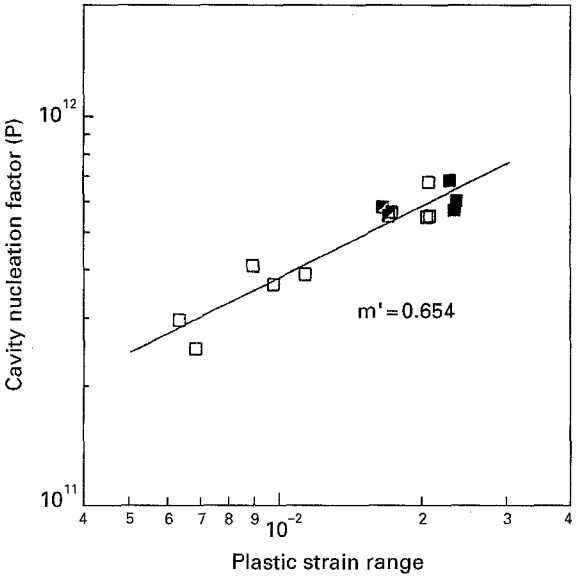

Figure 8 Variation of the cavity nucleation factor with plastic strain range for AISI 304 stainless steel. The data was recorded at (◩) 823 K, (□) 873 K and (■) 898 K.

a result of the dependence of the cavity nucleation factor on the plastic strain range in this alloy. The effect of temperature on the cavity nucleation factor is added to the temperature-induced change in the plastic strain range.

Using the new cavity nucleation factor, P', a comparison of the predicted lives with the experimental lives are shown in Figs. 11 and 12 for AISI 304 stainless steel and Incoloy 800, respectively. The predicted results are found to be be in good agreement with the experimental ones.

From the above considerations, it may be suggested that the cavity nucleation factor is only a function of the plastic strain range, and the effect of temperature is reflected by the change of plastic strain range induced by the temperature. That is, the cavity nucleation factor does not depend on the temperature itself at near 0.5 T_m.

3.3. New cavity nucleation factor as a material constant

It is generally believed that cavities are nucleated at geometrical irregularities on the grain boundaries where high stress concentration can be developed. In austenitic stainless steels the potential sites of stress concentration are the second-phase particles ($M_{23}C_6$ type Cr-rich carbides) precipitated on the grain boundaries during ageing treatment [10].

On the basis of the previously mentioned results, it can be assumed that the new cavity nucleation factor, P', is associated with the grain boundary precipitates acting as cavity nucleation sites. Therefore, the value of P' may have some specific physical characteristics which are represented by the number, distribution, size and/or kind of the grain boundary precipitates.

The purpose of this section is to discuss a physical meaning of the new cavity nucleation factor. In particular, an attempt has been made to find a

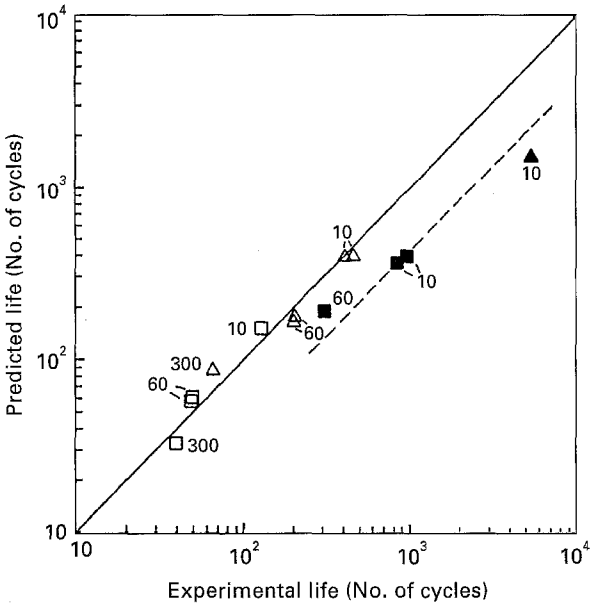

Figure 9 Comparison between predicted lives calculated from Equation 4 and experimental lives for Incoloy 800 stainless steel by Jaske *et al.* [11]. The data was recorded at; (△) 811 K, (□) 922 K and (△□) $\Delta\varepsilon_t = \pm 2.24$–$2.43\%$ and (▲■) $\Delta\varepsilon_t = \pm 0.53$–$0.54\%$.

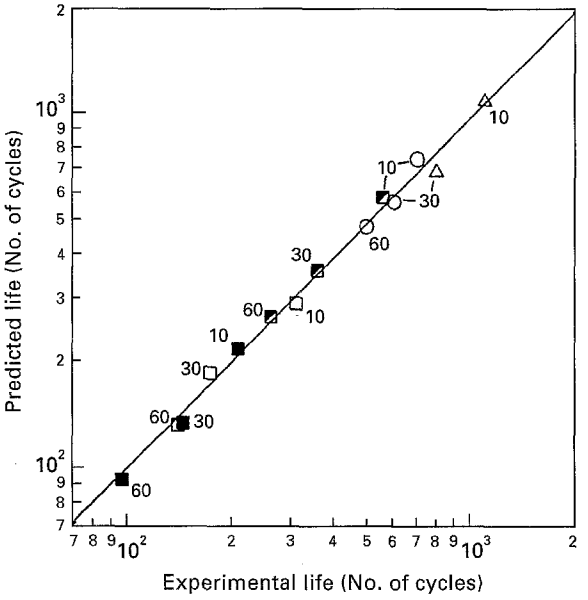

Figure 11 Comparison between predicted lives calculated from Equation 8 and experimental lives for AISI 304 stainless steel. The data conditions are represented by; (◩) 823 K, (□) 873 K, (■) 898 K and (□) $\Delta\varepsilon_t = \pm 2.0\%$, (○) $\Delta\varepsilon_t = \pm 1.5\%$ and (△) $\Delta\varepsilon_t = \pm 1.0\%$.

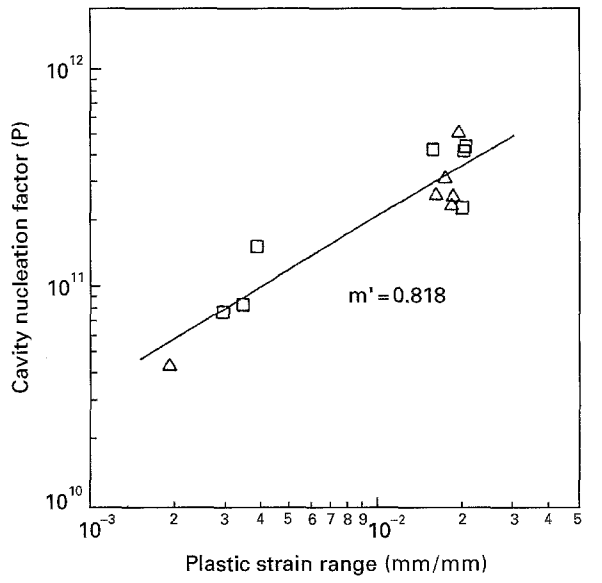

Figure 10 Variation of the cavity nucleation factor with plastic strain range for Incoloy 800 stainless steel by Jaske *et al.* [11]. The data were recorded at (△) 811 K and (□) 922 K.

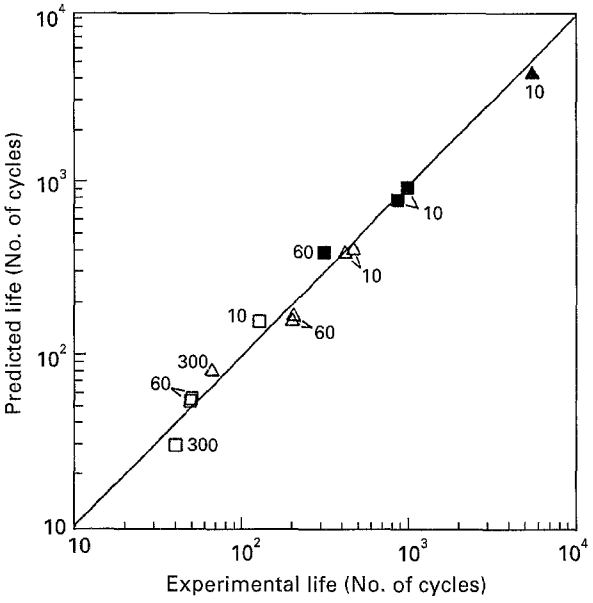

Figure 12 Comparison between predicted lives calculated from Equation 8 and experimental lives for Incoloy 800 by Jaske *et al.* [11]. The data were recorded at; (△) 811 K, (□) 922 K, (△□) $\Delta\varepsilon_t = \pm 2.24$–$2.43\%$ and (▲■) $\Delta\varepsilon_t = \pm 0.53$–$0.54\%$.

relationship between P' and the distribution of grain boundary precipitates.

In recent investigations, the authors of this paper reported that the addition of phosphorus to AISI 304L stainless steel is beneficial for the creep–fatigue life [14, 15]. In that work, they found out that phosphorus segregated on the grain boundary during solution treatment, that it retards grain boundary diffusion, and thus the precipitation of grain boundary carbides during ageing treatment is hindered. As the content of phosphorus is increased, the density of grain boundary carbides is found to be decreased. Therefore, these results can be used as an appropriate explanation of the relationship between P' and the characteristics of grain boundary precipitates.

Three experimental annealings of AISI 304L stainless steels which are based on a commercial grade type were produced in an induction furnace with the chemical compositions shown in Table V. For brevity, the three annealings will hereafter be called CSS, PSS1 and PSS2, respectively. The specimen preparation and creep–fatigue test procedures are given in detail elsewhere [14]. The specimens were solutionized at 1373K for 1h and aged at 1033K for 50h to allow the formation of a well defined grain boundary carbide that was stable during the subsequent experiments.

The typical grain boundary carbide morphologies of the heat treated CSS, PSS1 and PSS2 are shown in

TABLE V Chemical composition of commercial and P-doped type 304L stainless steels

Material	C wt %	Si wt %	Mn wt %	P wt %	S wt %	Cr wt %	Mo wt %	Ni wt %	Fe wt %
CSS	0.026	0.32	1.16	0.028	0.018	18.09	0.42	9.3	bal
PSS1	0.029	0.30	1.10	0.090	0.020	18.00	0.40	9.3	bal
PSS2	0.029	0.30	1.10	0.209	0.020	18.00	0.39	9.2	bal

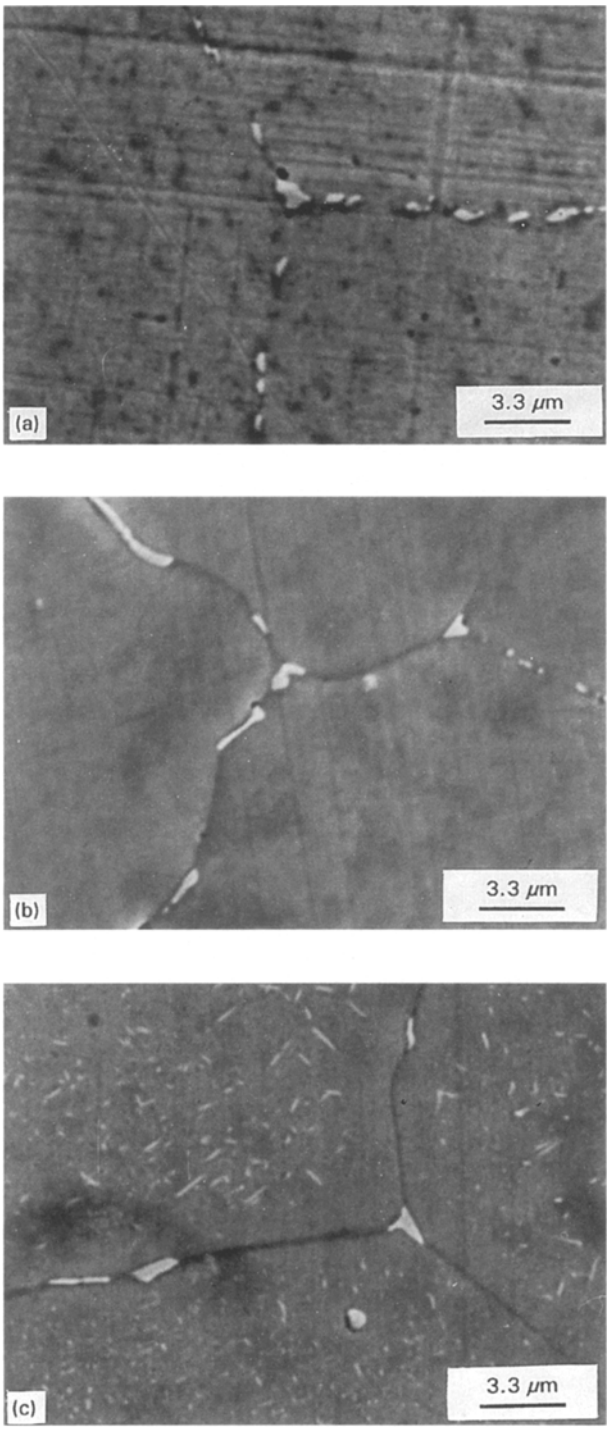

Figure 13 SEM micrographs showing the distribution of grain boundary carbides for three different AISI 304L stainless steels; (a) CSS (b) PSS1 (c) PSS2.

Fig. 13. From these illustrations one can easily and definitely see that as the content of phosphorus is increased, the density of carbides is decreased. To quantify the distribution of the grain boundary carbides, the linear density of the carbide was measured by an image analyser.

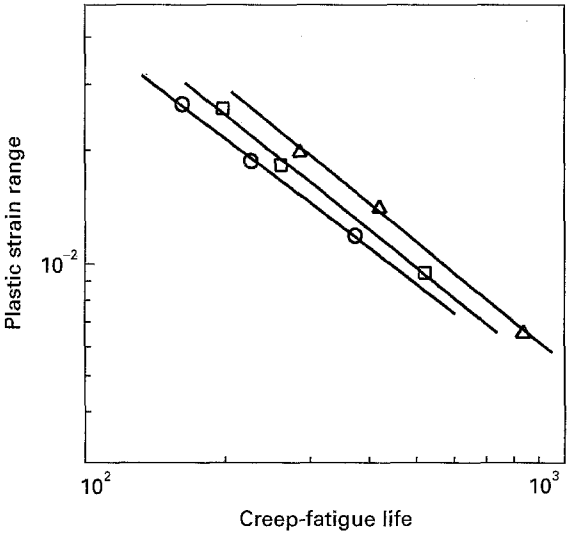

Figure 14 Coffin–Manson plot for three different AISI 304L stainless steels with tensile hold time of 10 min. The steels are; (○) CSS, (□) PSS[1] and (△) PSS2. The other conditions are $T = 823$ K, $t_h = 30$ min, $\dot{\varepsilon} = 4 \times 10^{-3}\ s^{-1}$ and an argon atmosphere.

In this section, the creep–fatigue test results of the three different phosphorus-containing alloys are briefly discussed. Some of these results have been previously published by the present authors [14, 15] and the others have been conducted especially for this study.

Fig. 14 shows the creep–fatigue lives of the three heats at various plastic strain values with a 30 min tensile hold time (i.e. a Coffin–Manson plot). From these results the interesting fact is observed, that the life under creep–fatigue condition over a wide range of plastic strain values increases with increasing content of phosphorus.

From the observation of the segregation of the phosphorus by Auger electron spectroscopy (AES) and LNT fractured surface of the creep–fatigue tested specimen, we could conclude that the phosphorus reduces the number of nucleated cavities by a reduction of the density of grain boundary carbides. That is, as shown in Fig. 13, the segregated phosphorus on the grain boundary reduces the number of carbides, which are precipitated during the ageing treatment and act as a cavity nucleation site. This reduction in the number of cavity nucleation sites results in the increase of creep–fatigue life.

Using the results of the creep–fatigue test shown in Fig. 14 and Table VI, the values of the cavity nucleation factor (P) are calculated to show that the cavity

TABLE VI Creep–fatigue test data for commercial and P-doped 304L stainless steel tested at 823 K

Material	$\Delta\varepsilon_t$ (%)	$\Delta\varepsilon_p$ (%)	$\int \sigma\, dt$(MPa sec)	N_{exp}
CSS	± 2.5	2.685	519690	158
	± 2.0	1.900	457140	221
	± 1.5	1.218	390435	365
PSS1	± 2.5	2.625	569160	192
	± 2.0	1.860	523440	255
	± 1.5	0.978	444705	513
PSS2	± 2.5	2.040	654870	279
	± 2.0	1.460	606090	410
	± 1.5	0.690	528510	827

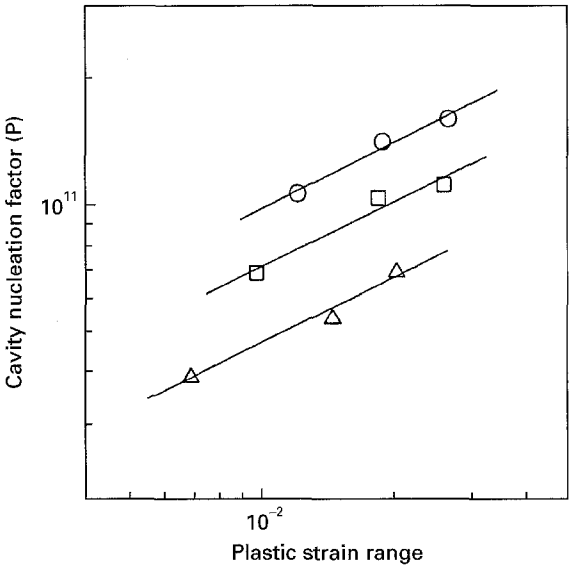

Figure 15 Variation of the cavity nucleation factor with plastic strain range for three different AISI 304L stainless steels; (○) CSS, (□) PSS1 and (△) PSS2. The other conditions were $T = 823$ K, $t_h = 30$ min, in an argon atmosphere.

TABLE VII The calculated parameters and linear density of grain boundary carbides

	Linear density of G.B. ppt (m^{-1}) $\times 10^5$	P' $\times 10^{11}$	m'
CSS	5.446	11.17	0.529
PSS1	3.010	7.526	0.511
PSS2	1.264	5.207	0.522

nucleation factor for the three heats also depends on the plastic strain range. These results are shown in Fig. 15.

The calculated value of P' and the linear density of grain boundary precipitates for the three materials are shown in Table VII. The value of P' and the linear density of grain boundary precipitates are simultaneously decreased with increasing phosphorus content. From these data, we obtain a relationship between the value of P' and the distribution of grain boundary precipitates. As shown in Fig. 16, P' is found to be closely related with the density of grain boundary precipitates giving a linear relationship between them.

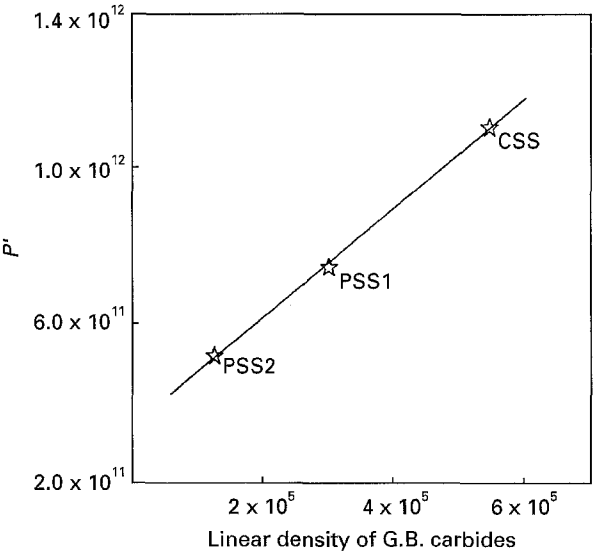

Figure 16 Relationship between the linear density of grain boundary carbides and new cavity nucleation factor, P'.

Thus, it is reasonable to conclude that the new cavity nucleation factor, P', is a material constant, which is associated with the characteristics of grain boundary precipitates. The significant meaning of this analysis is that the creep–fatigue life can be predicted by measuring the value of P' of a material, that is, if the P' can be obtained from the characteristics of the grain boundaries of a given material, then the creep–fatigue life can be easily predicted by use of the proposed equation without fatigue tests.

4. Conclusions

As a result of the phenomenological analysis discussed in this paper, important conclusions are made about the characteristic properties of the cavity nucleation factor;

(1) The cavity nucleation factor (P) introduced as a material constant in the previous model is found to be a function of the plastic strain range, but is independent of the testing temperature at near 0.5 T_m.

(2) Considering this dependency, a new cavity nucleation factor, P', is suggested and it is found to be a real material specific constant. Using this new factor a modified equation for creep–fatigue life prediction is proposed. The modified equation shows very good agreement between the predicted and experimental lives.

(3) The new cavity nucleation factor, P', which is newly regarded as a material specific constant, is found to be closely related with the density of grain boundary precipitates.

(4) If the generalized relationship between the value of P' and the characteristics of grain boundary precipitates of a given material are known, the creep–fatigue life can be predicted by measuring the density of grain boundary precipitates of a material.

Acknowledgement

The authors acknowledge the financial support of the ministry of science and technology (MOST) in Korea

which made this work possible through a cooperative research grant under the Korea–Hungary cooperative science program.

References

1. B. TOMKINS and J. WAREING, *Met. Sci.* **11** (1977) 414.
2. S. MAJUMDAR and P. S. MAIYA, *Can. Met. Q* **18** (1979) 57.
3. J. W. HONG and S. W. NAM, *J. Mater. Sci.* **20** (1985) 3763.
4. D. HULL and D. E. RIMMER, *Phil. Mag.* **4** (1959) 673.
5. R. RAJ and M. F. ASHBY, *Acta Metall Mater.* **23** (1975) 653.
6. J. WEERTMAN, *Scripta Met.* **7** (1973) 1129.
7. D. LONSDALE and P. E. J. FLEWITT, *Mater. Sci. Eng.* **39** (1979) 217.
8. A. M. ERMI and J. MOTEFF, *Metall. Trans.* **13A** (1982) 1577.
9. C. R. BRINKMAN, G. E. KORTH and R. R. HOBBINS, *Nuclear Tech.* **16** (1972) 297.
10. J. M. LEE and S. W. NAM, *Int. J. Damage Mech.* **2** (1993) 4.
11. C. E. JASKE, H. MINDLIN and J. S. PERRIN, *Trans ASME* (1972) 930.
12. W. J. OSTERGREN, in Proceedings of the ASME–MPC Symposium on Creep–Fatigue Interaction, New York, Dec. 1976 (American Society for Mechanical Engineers, 1976) p. 179.
13. R. A. PERKINS, R. A. PADGETT, JR. and N. K. TUNALI, *Metall. Trans.* **4** (1973) 2535.
14. J. J. KIM and S. W. NAM, in Proceedings of the ECF Fracture Behaviour and Design of Materials and Structures, Torino, Italy, Oct. 1990 (EMAS Press, U.K. 1990) p. 1217.
15. Y. C. YOON, J. J. KIM, D. M. WEE and S. W. NAM, *J. Korean Inst. Met. Mater.* **30** (1992) 1401.

Received 13 July 1994
and accepted 15 December 1995